Diamond C 1*s* core-level excitons: Surface sensitivity

Alastair Stacey,[1,*] Bruce C. C. Cowie,[2] Julius Orwa,[1] Steven Prawer,[1] and Alon Hoffman[3]
[1]*School of Physics, The University of Melbourne, Victoria 3010, Australia*
[2]*Australian Synchrotron, 800 Blackburn Road, Clayton, Victoria 3168, Australia*
[3]*Schulich Faculty of Chemistry, Israel Institute of Technology, Technion, Haifa 32000, Israel*
(Received 15 March 2010; published 15 September 2010)

The effect of surface termination on C 1*s* core-level bulk excitons found near the surface in single-crystal diamond is reported. By simultaneously recording bulk (total electron yield) and surface (partial electron yield) near-edge x-ray absorption fine-structure (NEXAFS) spectra with a range of single-crystal surface terminations, variable bulk exciton energy blueshifts and linewidth broadening were observed, most notably in the reconstructed single-crystal diamond. Investigation of polycrystalline diamond and ultrananocrystalline diamond films, using the same technique, allowed for a comparison between the reconstructed single-crystal diamond surface and nanodiamond bulk excitons. These findings suggest that surface-related effects can be misinterpreted as quantum confinement in some nanodiamond NEXAFS studies. Band bending is suggested as a possible contributor to these results.

DOI: 10.1103/PhysRevB.82.125427 PACS number(s): 71.35.Cc, 81.05.ug, 73.22.−f

I. INTRODUCTION

Diamond is gaining momentum as the material of choice for a variety of advanced electronic and photonic applications, including possible applications in quantum information processing[1] and high power electronics.[2] Much of this interest has been driven by recent advances in high-purity growth processes of single-crystal (SC) diamond,[3] as well as an increasing ability to control the growth of mixed carbon allotrope materials, such as diamondlike carbon and ultrananocrystalline diamond (UNCD) films as well as nanodiamonds. The diamond surface is interesting scientifically due to its ability to reconstruct, for example. There is also a strong need for well characterized and high-quality diamond interfaces and surfaces to support each of the above technological applications.

X-ray absorption spectroscopy is well suited for probing the electronic structure of different diamond surfaces and has already been applied to a variety of diamond materials. These include homoepitaxial crystals,[4] dc glow discharge diamond films,[5] UNCD films,[6] detonation nanodiamonds,[7] and meteoritic diamonds[8] to name a few. Near-edge x-ray absorption fine structure (NEXAFS) is increasingly being recognized as a useful tool in accurately measuring sp^2/sp^3 variations in diamond films,[6,9–12] and is exquisitely sensitive to surface states[13] and defect states.[14] Specifically the C 1*s* bulk core-level exciton in diamond has proven to be a useful indicator of crystalline quality and has been shown to be sensitive to even small amounts of ion-induced damage.[15]

The last decade has produced many studies and much contention relating to the exact energy and binding model for this core-level bulk exciton,[16–21] with some authors noting its similarity to the substitutional nitrogen donor in diamond.[18,22] There have been conflicting reports regarding the possibility of quantum confinement in nanosized diamond particles,[23,24] with multiple authors reporting size-dependent exciton and band-edge energy shifts using NEXAFS data,[8,23,25–29] despite some argument that the nanodiamonds of interest are usually too large to display a change in the band gap of the material.[24] One study has confirmed a gradual widening of the band gap in successively smaller diamond crystals,[30] however the unoccupied states appear to remain unchanged while it is the occupied states band edge which drops to lower energies. However, occupied states are not measured in NEXAFS only studies[31] and as such the origin of the reported bulk exciton energy shifts still needs to be explored.

Despite the apparent discovery of diamond's surface exciton,[32] one effect which has received little attention is the sensitivity of the C 1*s* core-level bulk excitons to the surface environment and specifically to different surface terminations. Band bending in diamond is already known to be very sensitive to the surface termination. Understanding the effect of surface termination on bulk excitons found near the surface (herewith referred to as near-surface excitons) is especially pertinent for nanodiamonds due to the significant proportion of near-surface carbon atoms being probed. To check this properly, in the context of diamond NEXAFS, a very careful study involving different surface treatments on the same diamond sample is required. In order to eliminate concerns about relative energy calibrations, bulk and surface information should be recorded simultaneously. This study aims to utilize the very high-energy resolution x rays from the Australian Synchrotron to investigate the effect of various surface terminations on near-surface excitons from the [100] surface of high-quality homoepitaxial diamonds. In order to directly compare the core-level bulk exciton resonances with those near the surface, simultaneous partial yield (PY) (surface sensitive Auger electron) and total yield (TY) (bulk sensitive drain current) NEXAFS measurements were conducted. Similar measurements were also made on polycrystalline and UNCD films for comparison of near-surface and bulk exciton resonance effects.

II. EXPERIMENTAL DETAILS

x-ray photoemission spectroscopy (XPS) and NEXAFS measurements were conducted at the Australian Synchrotron

using an elliptically polarized undulator capable of providing photons in the energy range between 90 and 2000 eV. The NEXAFS spectra were measured using a vacuum system consisting of four interconnected chambers: (i) a load lock with heating facilities, (ii) a preparation chamber, (iii) a chamber dedicated to the XPS and NEXAFS measurements and connected to the beamline equipped with an hemispherical analyzer, retarding field analyzer, fluorescence yield device and drain current capabilities (etc.), and (iv) a central chamber used for sample transfer, equipped with a sample cassette which could be loaded with multiple sample holders. The base pressure of the vacuum chamber where the XPS and NEXAFS measurements were conducted was measured to be better than 2×10^{-10} Torr.

The NEXAFS measurements were carried out in the 280–310 eV photon energy range in the partial electron yield (PEY) and total electron yield (TEY) modes. Since the mean-free path of high-energy electrons in diamond is short (about 1 nm for 200 eV Auger electrons), the PEY (Auger) signal from these electrons can yield only surface sensitive information. This can be compared to the total electron yield, which probes the "bulk" of the material. The PEY measurements were carried out by recording the intensity of secondary electrons above 200 eV using a retarding field analyzer as a function of incident photon energy. The TEY signals were produced by measuring the sample current as a function of photon energy, or where this was not possible the 8 eV secondary electron flux was monitored with the hemispherical analyzer. The TEY and PEY spectra were normalized by comparison with a TEY signal measured from a sputter cleaned gold sample. This cancels any contributions originating from carbon impurities present in the beamline, which contribute to changes in the energy-dependent photon intensity reaching the sample. Each measurement was carried out by increasing the photon energies in steps of 0.05 eV. The energy scale of all spectra was fixed such that the TEY signal of each scan displayed a bulk second band gap of diamond known to be at 302.4 eV. Due to the stability of the beamline's monochromator this energy calibration only required the same shift of 0.7 eV for all scans measured. The TEY and PEY spectra were recorded simultaneously such that surface and bulk information could be directly compared. The expected photon resolution of the system was better than 0.05 eV. XPS measurements were conducted with incident photon energies of 600 eV, providing for surface sensitive impurity and termination analysis. A hemispherical Phoibos 150-SPECS analyzer was used to record the XP spectra.

The two single-crystal diamond samples studied were a high-purity Element6 chemical vapor deposited (CVD) IIa and a natural IIa diamond (Drukker). The surfaces under investigation were commercially [100] polished and were prepared *ex situ* by solvent cleaning (methanol, ethanol, and isopropanol) followed by a hydrogenation step in an Astex microwave CVD reactor. Both samples were exposed to the hydrogen simultaneously at an estimated 1100 °C in a 100% hydrogen plasma at 150 Torr with 1400 W of continuous 2.4 GHz microwave excitation. The sample temperatures were measured with a two-color fiber-based pyrometer and cross-checked with a disappearing filament pyrometer.

The hydrogen plasma treatment step for each sample is not only important because it provides a hydrogen-terminated crystal baseline, and because the hydrogen plasma is a very effective way of cleaning contaminants from the surface, but also because the hydrogen is effective at etching any unwanted phases of carbon at the diamond surface, and essentially produces a "clean" pure diamond surface.

After hydrogenation and exposure to ambient conditions (for transportation) the CVD diamond sample was mounted on a high-temperature e-beam heated sample holder, with a K-type thermocouple in physical contact with the sample. Various surface terminations were studied, including oxygen dosing, which was conducted in the preparation chamber, as well as water exposure, at sample temperatures of room temperature and 200 °C, processed in the load lock. The water vapor was collected by a repeated process of freeze/thawing a container of Milli-Q water and pumping away gas impurities, with the final thaw vapor being collected in a bleed line attached to the load lock. The oxygen and water dosing was conducted at pressures of 2×10^{-5} mbar and 5×10^{-5} mbar, respectively. Prior to each of the above-mentioned dosing experiments the sample was heated to ~1000 °C in the preparation chamber, forcing noncarbon surface species to be driven off, and leaving a C=C reconstructed surface ready for reactions with the oxygen/water molecules, this was also conducted in the preparation chamber. The natural IIa diamond was placed on a resistively heated sample holder alongside an UNCD film and a hot-filament CVD grown polycrystalline sample for comparison. This UNCD film incorporates grain sizes 10–30 nm (Ref. 33) and from previous literature was expected to show a bulk exciton peak position blueshift when compared to the single-crystal samples. The polycrystalline film was 70–100 nm thick with lateral grain sizes 20–50 nm and was hydrogenated in the Astex reactor under the same conditions as the single-crystal CVD samples. All samples were *in situ* annealed to ~400 °C, in order to thermally desorb adventitious surface contaminants, prior to any measurements using the synchrotron. It should be noted that although different dosings were performed on the same sample surface, the exact history and order of these dosings are not expected to affect each separate result, because the ~1000 °C anneal step between each subsequent dosing is known to produce a well reconstructed, and atomically clean, crystal surface.[34] Although separate single-crystal samples could have been used for each dosing experiment, it was considered more critical for direct comparisons that the single-crystal NEXAFS spectra were taken from the same single-crystal surface, in order to eliminate crystal quality and defect-related effects.

III. RESULTS

Figure 1 displays the XPS spectra, recorded from all samples and surface terminations and calibrated such that the diamond C 1*s* peak sits at about 285 eV for each spectrum. The three as-received sample scans [hydrogenated SC, hydrogenated polycrystal (poly) and UNCD] show some silicon and oxygen contamination, most of which is expected to be present in the form of silicon oxides. Markers of these can be seen as Si(2*s*), Si(2*p*), and O(1*s*) photoelectrons. The recon-

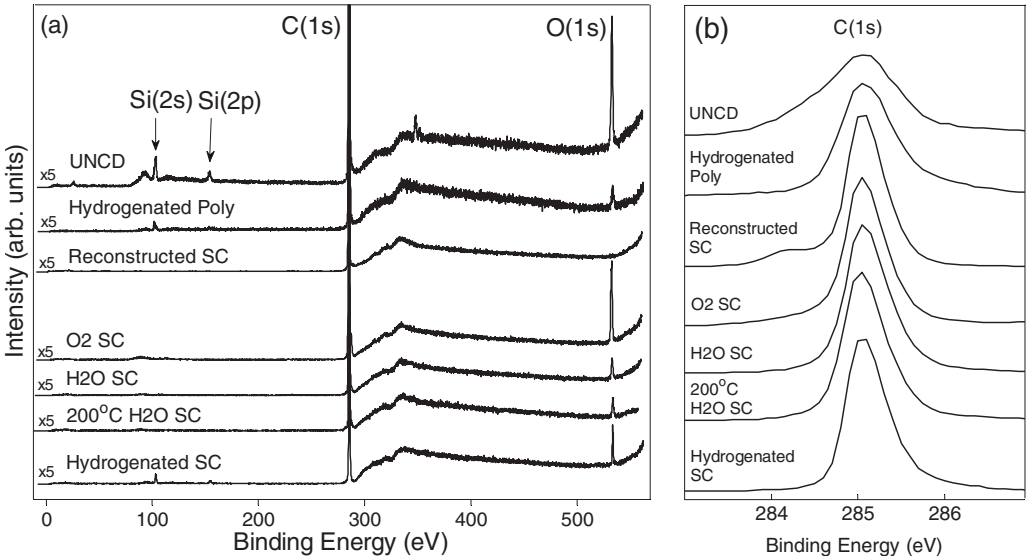

FIG. 1. (a) XPS spectra at 600 eV excitation photon energy from various diamond samples, normalized to the C 1*s* photoelectron peak area of each spectrum. Note the changes to surface-related impurity levels with different SC dosing treatments. (b) Zoom in of the C 1*s* photoelectron peaks.

structed SC surface spectrum shows no trace of contaminants, while a shoulder of the C 1*s* peak at around 284.2 eV is consistent with the expected monolayer of sp^2 hybrid bonded surface atoms, following the surface reconstruction. Each of the O2, H2O, and 200 °C H2O dosing procedures included a similar 1000 °C anneal step, resulting in similarly reactive and clean surfaces prior to dosing. Thus it can be seen that the O2- and H2O-related SC spectra can be used to identify the coverage of oxygen following dosing of each surface. Relative shifts in the C 1*s* binding energy were monitored, as different shifts could affect the measured NEXAFS peak positions from the different sample terminations. However uncontrollable charging effects make any such analysis extremely difficult from the XPS data, which is quite sensitive to sample charging.

NEXAFS spectra were recorded in both PY and TY modes for all prepared diamond surface terminations. The bulk sensitive TY absorption spectra are shown normalized in Fig. 2. Consistent with high-purity single-crystal diamond, the bulk spectra display very little pre-edge structure, indicating a low density of intraband unoccupied states. The sharp core-hole exciton peak occurs at 289.25 eV and a well-defined second absolute band-gap dip is seen at 302.4 eV. From Fig. 2(b) it can be seen that despite the respective spectra being recorded following different surface preparations and over a number of different days, the bulk exciton peak position remained entirely invariant. Surface sensitive PY spectra, as seen in Fig. 3(a), all show a similarly strong diamond conduction-band structure and near-surface exciton peak. This highlights the phase purity of the diamond crystal structure all the way to the very surface. The PY spectra include unoccupied states related to the surface termination of each sample and provide a wealth of information on surface bonding configurations, such as the clear C=C surface

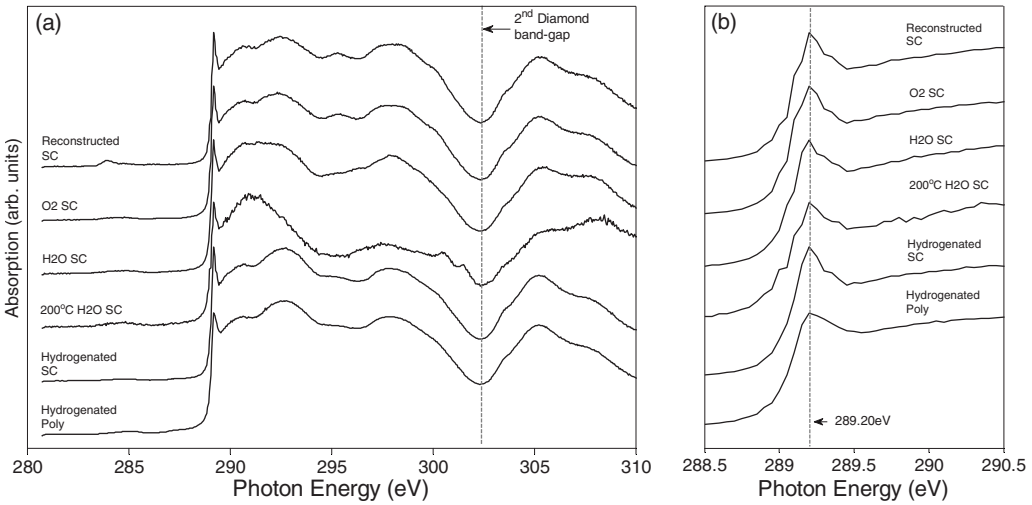

FIG. 2. (a) NEXAFS spectra recorded in the 280–310 eV photon energy range in the TY mode from different terminated single-crystal diamond surfaces. (b) Zoom in of core-level bulk exciton region, note the invariance of the exciton position to surface termination.

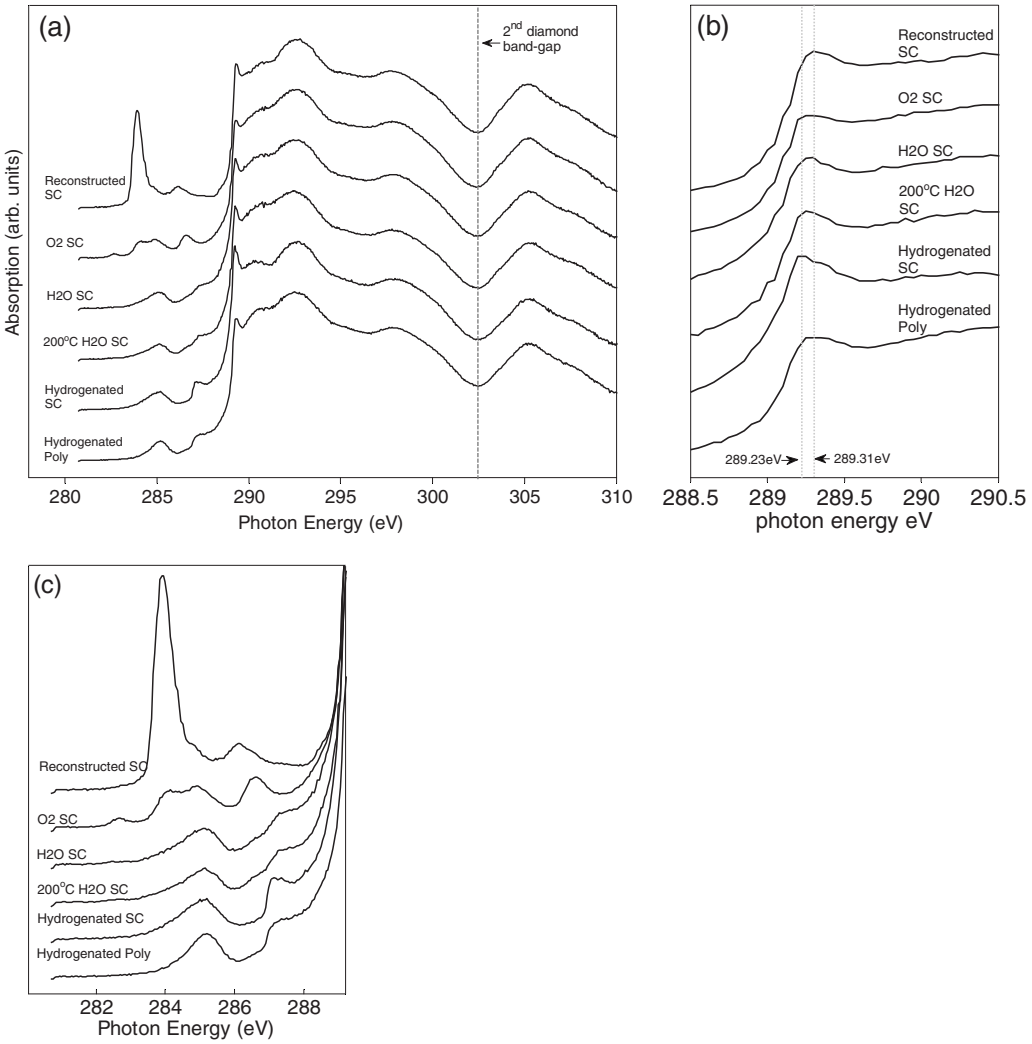

FIG. 3. (a) NEXAFS spectra recorded in the 280–310 eV photon energy range in the surface sensitive PY mode from different terminated single-crystal diamond surfaces. (b) Zoom in of core-level bulk exciton region, note the varying blueshifts with different surface terminations.

reconstruction signature following 1000 °C heating. Figure 3(c) shows the family of these unoccupied pre-edge peaks. Since each SC spectrum was taken from the same crystal surface and controllably dosed, these peaks can be unambiguously assigned to identifiable surface terminations. A focused study of these peaks will be presented elsewhere. When viewed closely [Fig. 3(b)] the near-surface exciton peaks from these samples appear to be broader than their bulk counterparts, and the peak positions (Table I) also display a termination-dependent blueshift, with the oxygen-related terminations and reconstructed surface producing, respectively, higher energy near-surface exciton peak positions than for the purely hydrogen-terminated single-crystal diamond surface. Of note is the exciton peak from the hydrogen-terminated surface which appears to be only about 0.03 eV higher in energy than its counterpart measured in the bulk. The three different surface treatments which are expected to result in some form of oxygen termination, namely, different water and oxygen exposures following surface reconstruction, appear to produce a relatively consistent exciton position. Here it should be stressed that the bulk and near-surface exciton signals were measured simultaneously in all cases. The bulk signals were also independently verified by simultaneously measuring the total yield with both

TABLE I. Diamond C 1*s* near-surface exciton peak positions for different SC surface terminations.

Diamond C 1*s* near-surface exciton	
Sample surface	Peak position (eV)
Hydrogenated SC	289.23
200 °C H2O treated SC	289.25
H2O treated SC	289.28
O2 treated SC	289.30
Reconstructed SC	289.31
Hydrogenated poly	289.30
UNCD	289.34
Diamond C 1*s* bulk exciton	289.20

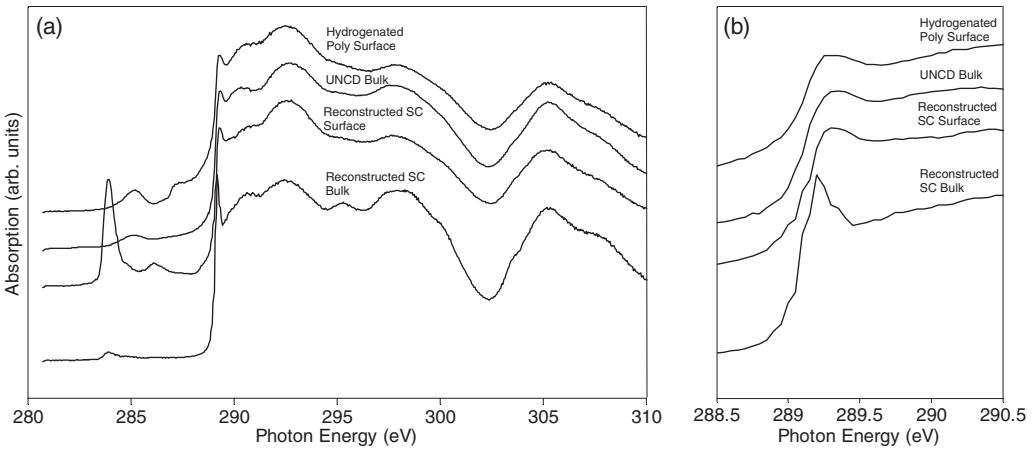

FIG. 4. (a) Comparison of bulk (TY) and surface (PY) NEXAFS spectra in the 280–310 eV photon energy range from a reconstructed single-crystal surface and the bulk spectrum from a UNCD film. (b) Zoom in of core-level bulk exciton region, note the similarity of the UNCD bulk signal to the single-crystal surface signal following thermally induced reconstruction.

the drain current and with the analyzer set to 8 eV secondary electrons while the surface signals were verified by measuring the partial yield with both a retarding field analyzer at 200 eV as well as the hemispherical analyzer set to the carbon Auger position of around 265 eV. This gives confidence that the recorded shifts, while small, are real.

The NEXAFs signal from the hydrogenated polycrystalline sample (Fig. 3) appears to be blueshifted at first glance, however upon closer inspection the exciton peak shape is irregular (flat) with some component near the hydrogenated SC position and higher energy components out to around the same position as the reconstructed SC surface.

The NEXAFS signal from the UNCD sample was recorded in bulk (TY) mode, and is compared with the bulk (TY) and surface (PY) signals from the ~1000 °C annealed single-crystal CVD diamond in Figs. 4(a) and 4(b). As can be seen in Fig. 4(a) the UNCD bulk spectrum shows a significant pre-edge feature at 285 eV, usually associated with sp^2-related π^* resonances. The CVD surface spectrum shows a significant peak at 284 eV indicating hybridized sp^2 bonding associated with a surface reconstruction. These different pre-edge features indicate that the exact nature of the chemical bonding at the vacuum and grain-boundary surfaces of these diamonds are not identical. Despite this, the UNCD bulk exciton peak characteristics and conduction band show a remarkable similarity with the "surface" scans from the reconstructed single-crystal sample [Fig. 4(b)], with the UNCD bulk exciton peak position being slightly blueshifted and broadened when compared with the reconstructed SC near-surface exciton. The reconstructed SC bulk exciton and hydrogenated polycrystalline diamond surface are also shown in these figures for comparison.

IV. DISCUSSION

The position and width of the near-surface exciton peaks recorded from the surfaces of single-crystal diamonds seem to be affected by surface termination, with the hydrogen-terminated surface displaying the smallest shift (relative to the bulk exciton) and the reconstructed surface displaying the largest blueshift and broadest peak width. Although it should be stressed that these are near-surface exciton peaks, not surface excitons at about 284 eV,[32] but are bulk excitons originating from carbon atoms close (~1 nm) to the diamond surface. Possible causes for these perturbations of the C 1*s* core exciton include exciton lifetime changes due to modification of the near-surface phonon spectrum and band bending known to occur near the surface (Fig. 5). The excited carbon atom's C 1*s* core level also lies spatially in the near-surface region, so any effect from band bending on the measured C 1*s* core exciton peak will only be observed if that core level is effectively screened from the band bending. Due to the finite size of the exciton wave function, and the potential gradient inside a band-bending region, the near-surface exciton peak would also be expected to broaden, if this effect was dominant. Although ensemble peak broadening is seen, the direction and magnitude of known band bending for hydrogen and oxygen terminated surfaces (order 1 eV) does not seem to be reflected in the exciton peak shifts measured here (order 0.1 eV). This may be due to a number of factors, not least of which could be photoinduced band bending initiated by the probing x rays. The resulting ordinary electron-hole pairs would likely react differently to the different surface terminations and provide a varying effect for each surface. Attempts to directly measure the C 1*s* core-level position, near the surface, with XPS did not yield any

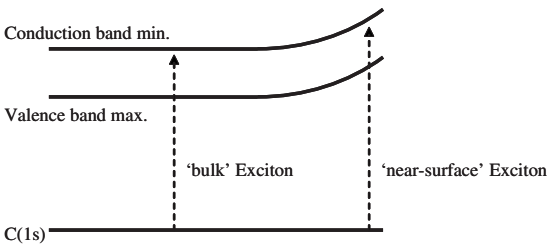

FIG. 5. Diagrammatic representation of the effect of band bending on core-level exciton energies measured in diamond in the bulk and near-surface regions, assuming no change in the C 1*s* core level near the surface.

useful information, due to unrecoverable charging-induced variations in the XPS spectra.

The magnitude of the measured energy shifts suggest no change in the binding model of these measured bulk excitons, at least in the loosely bound "final state" measured by NEXAFS. The relaxation to the tightly bound exciton state may be more affected by the surface proximity and termination, although this is not probed in this experiment.

It can be seen that the largest recorded blueshift from a (100) single-crystal surface is measured following full reconstruction. This is known to produce a hybridized sp^2 type bonding on the surface, with some similarity to the sp^2 hybridized shells and grain boundaries seen in various nanodiamond films. If we consider that the bulk NEXAFS data from the UNCD film mainly originates from near-surface carbon atoms, then it may be expected that the UNCD bulk exciton spectra will look similar to the "near-surface" excitons near reconstructed single-crystal diamonds. As can be seen in Fig. 4(b) there is a remarkable similarity between the UNCD 'bulk' exciton and the near-surface single-crystal exciton following surface reconstruction. Similarly the small-grain polycrystalline sample is expected to have hydrogen-terminated sp^3 surface components as well as interfaces between sp^3 grains and sp^2-like grain boundaries. This seems to be reflected in a broad and flat exciton peak with some lower energy components near the hydrogen-terminated SC exciton peak, as well as some high-energy component near the reconstructed SC peak energy. Thus it can be seen that the UNCD exciton, even when measured in the bulk mode (TEY) could more suitably be referred to as a near-surface exciton for comparisons with single-crystal surface scans.

It should be noted that the maximum near-surface exciton shift observed in these experiments is approximately 0.15 eV, which is less than some of the previously published blueshifts for nanodiamonds. This leads to the possibility that observed signatures of quantum confinement in suitably small crystals should be deconvolved from contributing surface termination effects, or that for small enough nanocrystals the surface termination effects might be strengthened as the effective surface area increases, thus producing a misleading indication of quantum confinement.

Due to the small shifts involved, and the closeness of some pre-edge features to the conduction-band edge, it is difficult to determine if the magnitude of the exciton binding energy itself is being affected in these crystals, or if the entire conduction-band edge moves. The latter would be consistent with band bending.

V. CONCLUSION

By carefully measuring high-resolution NEXAFS spectra, near-surface diamond C 1*s* core-level bulk excitons (near-surface excitons) are shown to be sensitive to the surface termination of each crystal. Blueshifting as well as spectral broadening were measured for a range of surface terminations, most noticeably following surface reconstruction to hybridized sp^2. Due to the near-surface proximity of all constituent carbon atoms, this effect is suggested to dominate the bulk core exciton blueshift results from some nanocrystal experiments, especially for crystals larger than 2 nm, effects which could be misinterpreted as quantum confinement.

ACKNOWLEDGMENTS

The authors would like to thank Dieter Gruen and Oliver Williams for provision of a nanocrystalline diamond sample for this work. This research project was carried out with the financial support of the Israeli Academy of Science and Arts, the Technion Fund for promotion of research and the Australian Research Council. A.H. was supported by the Australian Research Council during the project.

*Corresponding author; adstacey@physics.unimelb.edu.au

[1] J. Wrachtrup and F. Jelezko, J. Phys.: Condens. Matter **18**, S807 (2006).
[2] E. Kohn and A. Denisenko, Thin Solid Films **515**, 4333 (2007).
[3] F. Silva, K. Hassouni, X. Bonnin, and A. Gicquel, J. Phys.: Condens. Matter **21**, 364202 (2009).
[4] A. Hoffman, A. Laikhtman, G. Comtet, L. Hellner, and G. Dujardin, Phys. Rev. B **62**, 8446 (2000).
[5] A. Heiman, I. Gouzman, S. H. Christiansen, H. P. Strunk, G. Comtet, L. Hellner, G. Dujardin, R. Edrei, and A. Hoffman, J. Appl. Phys. **89**, 2622 (2001).
[6] D. M. Gruen, A. R. Krauss, C. D. Zuiker, R. Csencsits, L. J. Terminello, J. A. Carlisle, I. Jimenez, D. G. J. Sutherland, D. K. Shuh, W. Tong, and F. J. Himpsel, Appl. Phys. Lett. **68**, 1640 (1996).
[7] T. Hamilton, E. Z. Kurmaev, S. N. Shamin, P. Y. Detkov, S. I. Chukhaeva, and A. Moewes, Diamond Relat. Mater. **16**, 350 (2007).
[8] T. Berg, E. Marosits, J. Maul, P. Nagel, U. Ott, F. Schertz, S. Schuppler, C. Sudek, and G. Schönhense, J. Appl. Phys. **104**, 064303 (2008).
[9] J. Nithianandam, J. C. Rife, and H. Windischmann, Appl. Phys. Lett. **60**, 135 (1992).
[10] J. Díaz, S. Anders, X. Zhou, E. J. Moler, S. A. Kellar, and Z. Hussain, J. Electron Spectrosc. Relat. Phenom. **101-103**, 545 (1999).
[11] Y. Muramatsu, K. Shimomura, T. Katayama, and E. M. Gullikson, Jpn. J. Appl. Phys. **48**, 066514 (2009).
[12] F. L. Coffman, R. Cao, P. A. Pianetta, S. Kapoor, M. Kelly, and L. J. Terminello, Appl. Phys. Lett. **69**, 568 (1996).
[13] M. Lübbe, P. R. Bressler, D. Drews, W. Braun, and D. R. T. Zahn, Diamond Relat. Mater. **7**, 247 (1998).
[14] A. Laikhtman, I. Gouzman, and A. Hoffman, Diamond Relat. Mater. **9**, 1026 (2000).
[15] A. Laikhtman, I. Gouzman, A. Hoffman, G. Comtet, L. Hellner, and G. Dujardin, J. Appl. Phys. **86**, 4192 (1999).
[16] J. F. Morar, F. J. Himpsel, G. Hollinger, G. Hughes, and J. L. Jordan, Phys. Rev. Lett. **54**, 1960 (1985).
[17] K. A. Jackson and M. R. Pederson, Phys. Rev. Lett. **67**, 2521 (1991).

[18] Y. Ma, P. Skytt, N. Wassdahl, P. Glans, D. C. Mancini, J. Guo, and J. Nordgren, Phys. Rev. Lett. **71**, 3725 (1993).
[19] S. Tanaka and Y. Kayanuma, Phys. Rev. B **71**, 024302 (2005).
[20] S. Tanaka and Y. Kayanuma, Solid State Commun. **100**, 77 (1996).
[21] Y. Kayanuma and S. Tanaka, J. Electron Spectrosc. Relat. Phenom. **136**, 167 (2004).
[22] A. Mainwood and A. M. Stoneham, J. Phys.: Condens. Matter **6**, 4917 (1994).
[23] L. C. Chen, T. Y. Wang, J. R. Yang, K. H. Chen, D. M. Bhusari, Y. K. Chang, H. H. Hsieh, and W. F. Pong, Diamond Relat. Mater. **9**, 877 (2000).
[24] J.-Y. Raty, G. Galli, C. Bostedt, T. W. van Buuren, and L. J. Terminello, Phys. Rev. Lett. **90**, 037401 (2003).
[25] Y. H. Tang, Z. T. Zhou, Y. F. Hu, C. S. Lee, S. T. Lee, and T. K. Sham, Chem. Phys. Lett. **372**, 320 (2003).
[26] C. L. Dong, S. S. Chen, J. W. Chiou, Y. Y. Chen, J.-H. Guo, H. F. Cheng, I. N. Lin, and C. L. Chang, Diamond Relat. Mater. **17**, 1150 (2008).
[27] J. Birrell, J. E. Gerbi, O. Auciello, J. M. Gibson, D. M. Gruen, and J. A. Carlisle, J. Appl. Phys. **93**, 5606 (2003).
[28] Q. Yang, S. Yang, Y. S. Li, X. Lu, and A. Hirose, Diamond Relat. Mater. **16**, 730 (2007).
[29] Y. K. Chang, H. H. Hsieh, W. F. Pong, M.-H. Tsai, F. Z. Chien, P. K. Tseng, L. C. Chen, T. Y. Wang, K. H. Chen, D. M. Bhusari, J. R. Yang, and S. T. Lin, Phys. Rev. Lett. **82**, 5377 (1999).
[30] T. M. Willey, C. Bostedt, T. van Buuren, J. E. Dahl, S. G. Liu, R. M. K. Carlson, L. J. Terminello, and T. Moller, Phys. Rev. B **74**, 205432 (2006).
[31] T. M. Willey, C. Bostedt, T. Van Buuren, J. E. Dahl, S. G. Liu, R. M. K. Carlson, L. J. Terminello, and T. Moller, Phys. Rev. Lett. **95**, 113401 (2005).
[32] R. Graupner, J. Ristein, L. Ley, and Ch. Jung, Phys. Rev. B **60**, 17023 (1999).
[33] D. Zhou, D. M. Gruen, L. C. Qin, T. G. McCauley, and A. R. Krauss, J. Appl. Phys. **84**, 1981 (1998).
[34] M. Nimmrich, M. Kittelmann, P. Rahe, A. J. Mayne, G. Dujardin, A. von Schmidsfeld, M. Reichling, W. Harneit, and A. Kühnle, Phys. Rev. B **81**, 201403(R) (2010).